Webology (ISSN: 1735-188X)
Volume 18, Number 6, 2021

Effective Heart Rate Estimation From PPG Signal By Fuzzy Wavelet Approach

Ameena Firdous Nikhat[1] , Dr Shameem Akhter[2]

[1]Department CSE Khaja Banda Nawaz College of Engineering Gulbarga University.

[2]Professor Department CSE Khaja Banda Nawaz College of Engineering Gulbarga University.

ABSTRACT

Wrist wearable devices have become part of one's daily requirement to track an individual's heart rate, to keep a track of various health-related disorders. While a person is, exercising his heart rate may shoot up and give a false value due to the motion artefacts associated with it. Our main aim here is to reduce the motion artefacts to give an accurate heart rate. The PPG signal emits light, which is absorbed by the skin and a photodiode, which records all the changes in the bloodstream. PPG signal extracted from the photodiode is corrupted by the motion artefacts many algorithms are proposed to lessen motion artifacts we have proposed a deep learning technique to lessen the motion artefacts and denoising PPG signals. The PPG signal is extracted from the ECG signal considering a dataset, which is further preprocessed to clean the contaminated PPG signal. Denoising the PPG signal as a well-performing spectral examination to get a clean PPG signal. We perform feature extraction where all the necessary information is extracted and processed. PPG is extensively used owing to its being economical. Research is being done to extend the features of PPG to find the respiration rate, blood oxygen saturation. PPG signals work as a good alternative to ECG signals however, ECG signals give accurate values. We try to increase the effectiveness of our model to give accurate estimations for the detection of heart rate. The growth of wearable wrist devices has led to the innovation of acquiring clinical data.

Keywords: PPG, ECG, Denoising, Motion Artifacts.

1. INTRODUCTION

Estimation of accurate heart rate is a major concern these days as there are many chances of getting an erroneous result from PPG sensors due to motion artefacts (MA), our main aim here is to reduce motion artefacts to an extent to get an accurate heart rate. MA can be reduced by using various

algorithms like a priori algorithm; all these algorithms are used to reduce the error introduced by motion artefact. PPG signals go hand in hand with sensors in wristwatches to measure the heart rate while performing physical activity.

A photoplethysmogram emits a light signal to measure the heart rate and a photodetector that measures the heart rate back forth. These days even the younger generation is at risk of cardio, vascular diseases hence it is essential to keep track of blood flow, respiration rate, and oxygen saturation in the bloodstream. ECG signals are extracted by placing sensors on the chest as this process is tedious people are opting out for wrist wearable devices like smartwatches to track the heart rate. Motion Artifacts can corrupt the PPG signal while a person is doing some physical activity; our main goal is to determine accurate heart rate by reducing the background noise from the PPG signal.

In comparison with ECG signal, PPG is more economical and convenient to use whereas in the case of ECG signal it gives an accurate value PPG is more commonly used as it is embedded in smartwatches to estimate the blood flow, oxygen saturation. In terms of accuracy and power consumption ECG, signals are most accurate for measuring overall cardiac activity. The challenges associated with PPG is that is affected by cancelling varied light conditions as well as different skin conditions alongside motion artefacts. PPG gives an accurate value where the concentration of blood vessels is more hence, it is necessary to place a PPG sensor in the appropriate place.

With prolonged use of sensors, it may result in skin variations for persons with underlying skin conditions, ECG sensor can operate without the user's participation whereas PPG sensor requires the user's active participation as in a wearable wristwatch. PPG sensor in the wearable device is easy to install and convenient to use. The cardiac activity originating from the sinoatrial node is influenced by the electrical signals giving information about the heart activity. As the PPG signals are recorded daily, we can generate a screening of ECG activity, thus combining the convenience of usage from PPG and better accuracy of ECG making it easy to use as well as making it more reliable.

Input to the PPG signals is a sequence of time signals and the resulting output consists of a sequence of physical functions. Here we use a machine learning technique to train the data to determine the ECG interval from selecting the attributes of the PPG signal. In this model, we design a method, which can train several classifiers with preprocessed ECG and PPG signals which results in a set of signals we then segment these signals into cycles which in turn maps the corresponding PPG activity with the ECG activity.

The proposed model here helps in better understanding of ECG and PPG signal, the resulting signal is the same in comparison with the referenced ECG signal. It provides a better understanding of the two ECG and PPG signals, a model to reconstruct ECG signal to PPG signal. PPG works on the principle of the pulse oximeter. Keeping track of the heart rate helps us in knowing the cardiovascular activity of the heart it is recorded that during any physical activity the heart rate increases resulting in a false result, our main aim here is denoising the PPG signal to get

an accurate value to track the heartbeat per minute. The PPG signal is contaminated by motion artefact (MA) thereby giving an inaccurate value. In this paper, we focus on estimating clean PPG signals from wrist-worn devices and implementing an algorithm to reduce the motion artefact (MA).

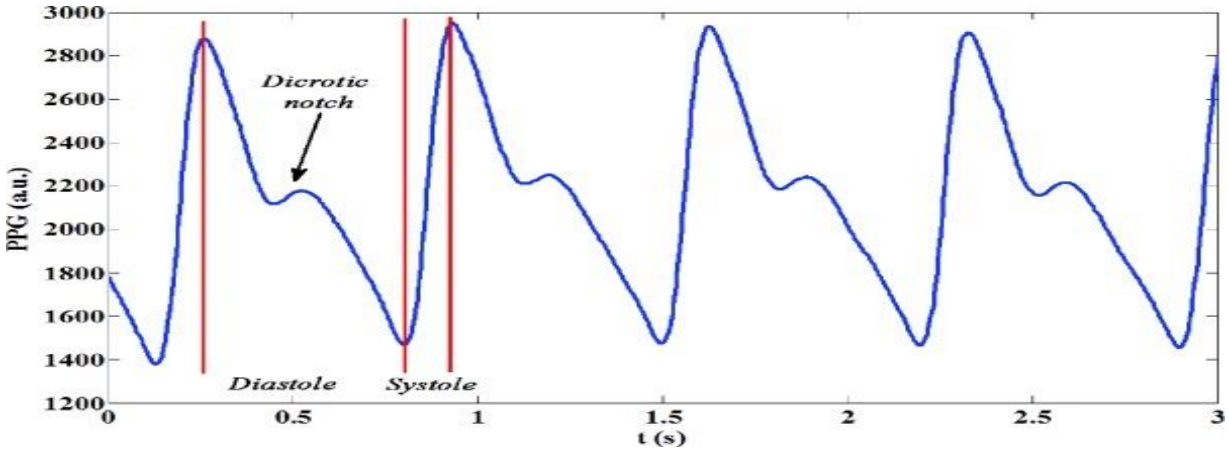

Fig 1. Sample PPG signal

When the PPG signal travels through our body it may interact with the blood flow. After a particular heartbeat. The muscles surrounding the heart need to split for the heart to beat again and the electrical signals may halt for a while for this to happen. We first preprocess the PPG signal and then align them into different pairs the data is fed to the training phase; we segment the data into different cycles. As the data from segmentation is modelled into different cycles, we then segment these into two cycles of equal length; we then normalize the PPG and ECG signals.

Motion Artifacts occur because of the movement of the sensor on the wrist-worn devices when a person is performing any physical activity or when the sensor is deformed based on its daily usage. The variations in the blood flow are due to many factors like the amount the intensity of the flow of blood and various other skin conditions, the wavelength of light absorbed by the skin etc.

Initially, the contaminated PPG signal from (MA) is fed to a filter that will preprocess the data from the signal and then the pair of data is segmented into different cycles. Statistical analysis is performed where the degree of certainty is determined, then the signal is checked for the quality to determine the presence of motion artefact if (MA) is detected then it is reduced by optimization algorithm and then the threshold is updated upon further filtering we get the required output.

In our proposed model, we have two steps, the first stage is the training phase the second stage is the testing phase. In the workflow training phase, the data is first preprocessed then the features are extracted using the feature extraction method the features extracted are then normalized then fed back into a classifier for the arrangement of the relevant features. During the testing phase, the data is preprocessed, which is then filtered with a filter and then it is labelled for

classification. The PPG sensor analyses the heart rate and tries to predict the outcome of the patient's health.

2. RELATED WORK

Physiological changes that happen in a person's body are used to determine a patient's overall health, changes in cardiovascular activities, oxygen saturation in blood, blood pressure, diabetes. This can be recorded based on contactless methods like using a PPG sensor to track the heart rate. In [3] they have developed a model; a deep learning-based contactless method is used to determine the heart rate. Wrist-worn devices provide a cheap alternative to track the health of a patient. Various types of sensors are used to detect blood glucose levels, temperature sensors, heart rate detection sensors, sensors to measure oxygen saturation. By combining IoT and cloud, computing healthcare monitoring systems are developed. To monitor basic symptoms, the physician can connect with the patients using Wi-Fi, message services, Bluetooth transferring data from sensors to mobile applications. To monitor the blood glucose level [8] through a smartphone, the patient's data is collected and stored in the cloud then by feature extraction they are segmented into three categories like normal, borderline and emergency cases. In [6] a respiration-monitoring framework was developed using sensors, data is collected using hardware and transmitted to the PPG signal, which is then analyzed to get the approximate respiration rate. By combining artificial intelligence and machine learning many techniques are developed using IoT healthcare systems. Le et al [9] developed a system based on IoT to keep track of novel coronavirus; here patient's clinical data is collected from various IoT sensors the data is stored on the cloud by removing noise covid 19 is detected. Ali et al [14] proposed a system for predicting heart diseases using ensemble learning, the features are extracted and fused to collect the data and predict heart disease. Software architectures like COTS are used as user interfaces to different users and applications. In [7] PPG signals are the most economical and cost-efficient method to detect the patient's heart rate from wrist wearable sensors, but these signals are sensitive to motion during physical activity resulting in an inaccurate value. In [15] data is collected from two PPG sensing devices and simultaneously collected three-axis accelerometers together mounted along with PPG sensor. The algorithm used here states that the data is first preprocessed estimating the (MA) and heart rate. Then filtering it further to get the desired result and then classifying them based on their previous task list for the activity to be performed. In the classification, phase the degree of contamination in the PPG signal depends on the extent of physical activity whether it is highly intense or less intense. The strength of the activity is proportional to (MA) contaminating the PPG signal.

A heart rate estimation algorithm based on decomposing the contaminated PPG signal into useful parts and classified into various parts to improve the accuracy. In [11] the effect of motion artefact can be reduced by optimization algorithms. The slight motion of the body results in the form of motion artefact affecting the result obtained. In this model, the input is a contaminated PPG signal along with the three-axis accelerometer in three directions in the next step denoising is done using adaptive Fourier decomposition. The spectrum is reconstructed using (MA) removal algorithm the resulting output heartbeat is estimated in beats per minute (BPM). In the next phase,

the magnitude of the signal obtained is subtracted to estimate the noise that is there in it. A conjugate-based method is used to stabilize the equation. Here in this paper AFODSS algorithm is proposed to determine the heartbeat of a person by denoising the PPG signal to remove the (MA). By combining AFODSS along with IoT to develop a framework for detailed analysis of wrist wearable devices. The time complexity of the algorithms is as well utilized for the one giving the maximum computation. In [1] a deep learning-based technology for denoising contaminated PPG signals, a CNN based approach is used to train the dataset recorded for 12 individuals. ECG signals determine cardiac activity using sensors, which are placed on the chest, whereas PPG sensors can be used on the wrist-worn devices in smartwatches making it more economical. The output result of noisy PPG reaches many peak values in comparison with a clean PPG signal where we can see a single peak in value. In this Deep, learning-based algorithm the first stage is preprocessing which is then passed on to a filter that will reduce noise then a sliding window is used to segment the frames, a deep CNN based technique is used for denoising the signal. The contaminated ECG signal can be used in determining the PPG signal.

This Deep Learn algorithm is used to train corrupted PPG signals along with clean PPG signals to train the algorithm, in this paper (MA) are reduced to an extent thus improving the accuracy in estimating the heart rate of a person during physical activity. In [8] using wireless sensors body wearable devices are minimized for effective use for determining the cardiovascular activity used as an alternative to ECG. In this paper [15] a Cor NET based technology for estimating the heart rate using one PPG signal recorded in random conditions based on the principles of Deep learning.

A deep learning model is used which are segmented into regression and classification layers. The relationship between ECG and PPG layers is detected. The Cor NET based technology combines Cor NET with the LSTM technique to estimate the heart rate using 22 PPG signals. Research is carried out in building energy-efficient techniques to determine the heart rate. Wireless sensors are revolutionizing the use of wearable devices to estimate heart rate such as fitness bands, smart watches. In [18] a wiener filtering method is proposed for sensing the heart rate from a contaminated PPG signal by reducing the (MA) along with measuring the three-axis acceleration signal. Wiener filtering technique is employed to denoising the PPG signal by reducing the error by comparing it with the desired signal and estimating the accurate heart rate. This proposed algorithm shows the least error rate in comparison with the existing algorithms for estimating the accurate heart rate by using the wiener-filtering technique, concluding this as the reliable method to estimate the heart rate. These devices play a vital role in tracking patients' health and help during the process of treatment of patients.

Deep learning-based technology is used to estimate heart rate instantly by using PPG sensors thereby reducing motion artefacts. In [16] a deep learning neural network is used which combines convolutional layers along with LSTM, three connected layers, a deep learning framework is built to use power spectrum of light from PPG signal using three-axis acceleration signals. The resulting

power spectrum and three-axis acceleration signal to determine accurate heartbeat from a PPG signal.

It has been shown that when the recovery rate is less, after a physical exercise there exists a possibility of coronary artery disease. Three to four wearable devices on the wrist are used to record the reading from medium to high rigorous activity the heartrate estimation with least error rate. In [13] a deep learning algorithm is proposed that approximates heart rate by (systolic blood pressure and diastolic blood pressure) using a convolutional neural network for feature engineering making it cost-effective. Estimating the large population affected by cardiovascular devices increase the performance of the proposed system suffering from cardiovascular devices and strokes.

The proposed framework here has three stages one is processing, second is the model-building phase third is the training and testing phase. A pp-net technique is proposed here that estimates the heartbeat along with blood pressure using a single PPG sensor. The feature extraction-based approach is used that saves the cost from feature extraction and feature selection process making it easier and cost-effective to use. In [19] a TROIKA based framework is used which works best with motion artefacts and denoising the PPG signal based on spectral tracking. The input data is fed to a band pass filter then the signal is broken down to a simpler format from a complex form. Then the signal is passed to a temporal difference to predict the future value of a signal from a small value. TROIKA works on a single bandwidth of PPG signal passed on to spectral peak value detector to get the desired output, providing more flexibility to wrist-worn devices. In [2] the reconstruction of PPG signals from ECG based on the model constructed and data accumulated. Measuring PPG signals from ECG signals from signal processing system for easily obtained PPG data. The changes in the blood volume can also be detected from PPG associated with each heartbeat. an efficient feature extraction method is used for hand movement recognition. Extracting the features collecting based upon the pattern recognition method for extracting features and segmenting the data based upon different hand movements.

An artificial neural network layer is used to model a classifier to categorize different features. Reducing the dimensionality of data to improve feature selection using principal component analysis technique for accurate feature selection. To enhance the entire performance of the feature selection process. Improvising the method for different hand movements as well. Based on different hand movement recognition to determine the exact heart rate by reducing motion artefacts and improving the overall performance of the system.

3. PROPOSED SYSTEM

PPG sensor is used in wrist-worn devices to measure heart rate, blood flow, and oxygen saturation. However, they suffer from motion artefacts (MA). PPG signals of varying wavelengths are used towards the removal of motion artefacts (MA) in determining the exact heart rate. PPG sensors used in wearable devices may be costly difficult to use, hence making it more economical and user friendly in our proposed system.

In the proposed model, the heart rate estimation based upon the PPG signal is classified into three stages, in the first stage preprocessing of the dataset, combining it with a 3-axis accelerometer signal. Statistical analysis of the resulting dataset, which is then passed on to a band, pass filter for (MA) reduction.

Algorithm 1: Heart rate estimation algorithm from PPG

1. Initialize
2. Pre-processing the dataset obtained from the PPG signal
3. Combine it with 3 axis accelerometer signals
4. Statistical analysis of the resulting bandwidth
5. Applying (MA) reduction band pass filtering technique
6. Down sampling of the dataset after (MA) reduction
7. Estimating the heart rate from wavelength tracking
8. Accurate Heart rate obtained after normalization.

The PPG signal consists of noise, for effective estimation of heart rate we intend to decrease the noise associated with the PPG signal. Along with the three-axis, the accelerometer signal is used with the corrupted PPG signal to reduce the motion artefact from the signal.

$$x(n) = \alpha_a^D(\theta)\ u_a(\theta - 1) + \alpha_b^D(\theta)u_b(\theta - 1) + \alpha_c^D(\theta)u_c(\theta - 1) \quad (1)$$

Here the equation for the thee-axis accelerometer signal is given where a, b, c determine the three axes in three directions. This is used as the input along with the contaminated PPG signal is fed to a filter to decrease the motion artefact (MA) and hence to extract a clean PPG signal.

2. There are three phases in this algorithm first we perform feature engineering, second is preprocessing, classification, pattern recognition.

The first step here is feature engineering where the features are extracted based upon the data available; to speed up the number of iterations we use the PCA method to reduce the dimensionality of large datasets into smaller ones. This data is fed onto an ANN classifier where the classification occurs with artificial neural networks

Feature extraction is done using the following equation:

$$F(\emptyset, g) = \int_{-\infty}^{+\infty} v(\theta)\ \frac{ge}{2\pi}\ -\frac{(a-\theta)g2}{2}\ e^{-2\pi g\theta} d\theta \quad (2)$$

Here θ represents the duration, g represents the wavelength, a is the window function. The raw data signals are segmented into different signals. These signals are segmented into a matrix of time across frequency. The PCA method is used for dimensionality reduction where the large data sets obtained are converted into smaller data sets. PCA has an important advantage in classifying the

features based on their importance. This serves as the desired input for pattern recognition, in pattern recognition, which is used to recognize patterns in raw data depending on the similarities in the collection of large data sets. The phases in pattern recognition include sensing the input obtained from the raw data, and then the data is segmented, then features are selected based upon the other clusters, classification based on the clusters then we process the data before the output is generated.

PPG signals are recorded during the movement of muscles; these signals as well consist of noise, which needs to be reduced to get an accurate result. These signals are detected from the surface of the skin. The data here is collected based on six hand movements bypassing the EMG signals. The frequency, power spectral density value, mean frequency and peak frequency is calculated. To check the performance of EMG features we use class reparability. Then we perform statistical analysis to separate the data into two classes. We estimate the performance of the algorithm based on six hand movements while closing the hand, opening the hand, extending the wrist, flexing the wrist, hand firm and relaxed positions.

The difficulty here is to differentiate the feature vector to cluster the EMG signals based on their relevant subject depending, as they are associated with noise. A feature vector is important here because it affects the accuracy of the model. Here we use ANN based classification model which uses a multilayer perceptron-based feed-forward network.

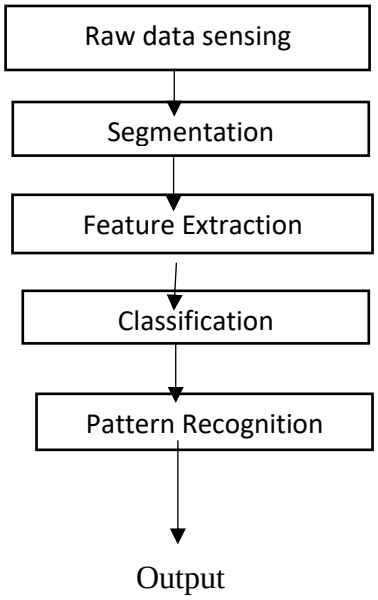

Fig 2: Block diagram for MA removal

The fuzzy wavelet-based packet algorithm:
Step 1: For each signal, maximization of a full wavelet packet-based decomposition.

Step 2: Construct fuzzy set-based packet wavelength and compute the value of entropy.
Step 3: Select the optimal solution corresponding to the maximum value estimated.
Step 4: Sort the elements in descending order with subspaces in between them.
Step 5: Inherit directly or indirectly to remove the k value from the x set.
Step 6: The set consists of a feature-based packet wavelength decomposed set.

The algorithm used here is used to extract features for optimizing the wavelength packet transform algorithm. To extract features for every channel connected along with each other that is used for the classification model.

In a collection of signals, the feature vector is applied for each set of data from each cluster to make it a tree of the 'i' level of decomposition. Then performing normalization of the decomposed subset, which is then passed on for filtering the required energy level, hence normalizing the feature vectors.

$$T\sigma_{i,j} = \log\left(\sum a\left(\frac{x_{i,J}^{Y} a^{y}}{\frac{A}{2^{i}}}\right)\right) \quad (3)$$

4. Mutual information estimation for fuzzy wavelet:

MI is used to determine the dependency between various random number variations. The result is highly uncertain. MI approach is used to strengthen the model, maximizing the MI estimation capacity between each random variation, we use an algorithm like the k-nearest neighbour algorithm. The amount of information measured in entropy is to measure the degree of uncertainty.

Let us consider, $q = \{q1, q2 \ldots \ldots \ldots qn\}$, the fuzzy wavelet value is given as a set consisting of the patterns, and to describe the jth vector, the fuzzy wavelet value is given as:

$$E_{xj} = \left(\frac{R_x - R_J}{t+\theta}\right)\frac{2}{N-1} \quad (4)$$

In this equation, N is the fuzzy set parameter, and $\theta > 0$ is a less value to ignore its computation. x is a discrete random variable consisting of the fuzzy sets zr to a.

$$S(a, zr) = \frac{\sum j \in B - E_{xj}}{DS} \quad (5)$$

We build a fuzzy wavelet set by selecting each feature which will then set a mirror image on the class group which adds the features to the sample dataset. The substitute of the fuzzy wavelet to get a probability function which trains the patterns belonging to that particular class group.

$$X(a, Z_r) = -S_{azr} \log S_{azr} \quad (6)$$

Here the $X(a, Z_r)$ can show that the extent to which the sample can be described which belong to a class group x which will provide the relevant information to that particular group.

$$X(a, W_r) = \sum_{X=1}^{Z} \quad X(a, Z_r) \tag{7}$$

The training dataset that belongs to the class group and DS is the collection of patterns set. The fuzzy entropy wavelet value is given as $X(a, W_r)$ given.

$$S(zr) = \frac{\sum_{F \in B, \forall v} E_{xj}}{DS} \tag{8}$$

For calculating the entropy value amongst all the classes, the entropy value has to be summed up to get the set to obtain a set of fuzzy entropy $X(a, W_r)$.

$$Q_{\sigma\, x,y} = \left(\frac{\sum_z Y_{x,y,z}^{\theta} R}{\frac{C}{2^X}} \right) \tag{9}$$

The entropy set defined satisfies all the conditions and is known as the joint functional fuzzy wavelet. The equations are applied to each sample group to determine each feature that is gathered to get the set to satisfy the entropy.

$$A_x = \frac{G(N; a_x)}{Ja_x} \tag{10}$$

The proposed algorithm extracts feature based on the entropy value which should then be normalized and submerged into a subspace. The normalized packet wavelet value is used for classification.

5. EXPERIMENTAL ANALYSIS:

The main benefit of using our proposed method is to overcome the fluctuations which come across a PPG signal. We perform a spectral examination for every subject to find the fuzzy wavelet value for each parameter by seeing each frame. In the first step of the experiment the performance value of which technique is evaluated. We perform Feature extraction for evaluating the entropy value to select a feature suitable to detect the fuzzy wavelet packet. In the second phase we perform classification, we also find the MI value. A windowed approach is used to sense the probability of the joint distribution. We compare the result with the ground truth value for subject 4 and subject 10 of the ISPC SPC dataset. We calculate the Pearson correlation as well as mean absolute error, we can conclude that our model is working better in comparison with the existing system. We have calculated values for rmse, Mae, and standard deviation.

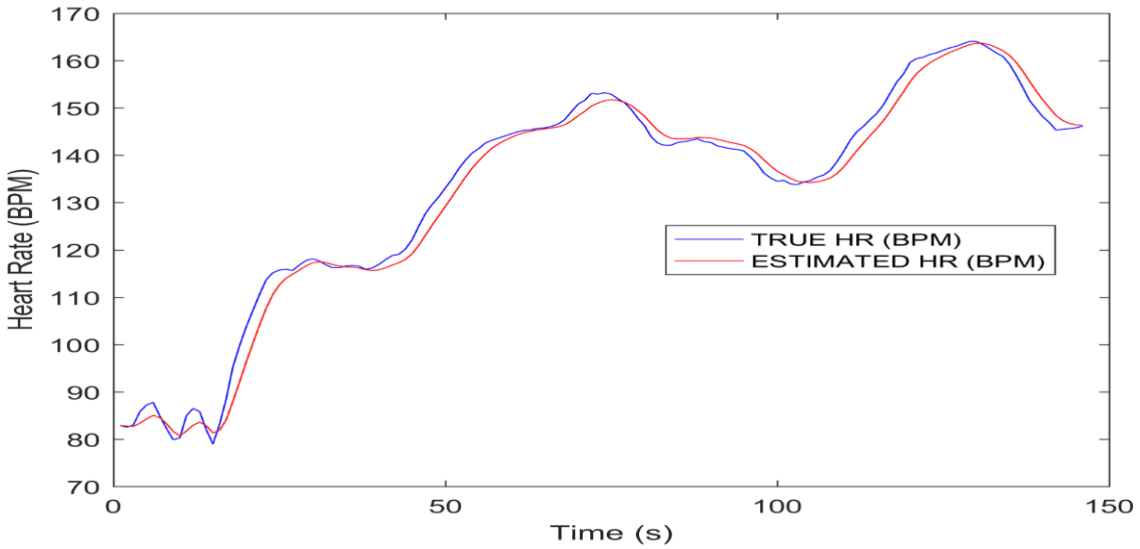

Fig 3: Comparison of estimated HR with ground truth of SUBJECT 4

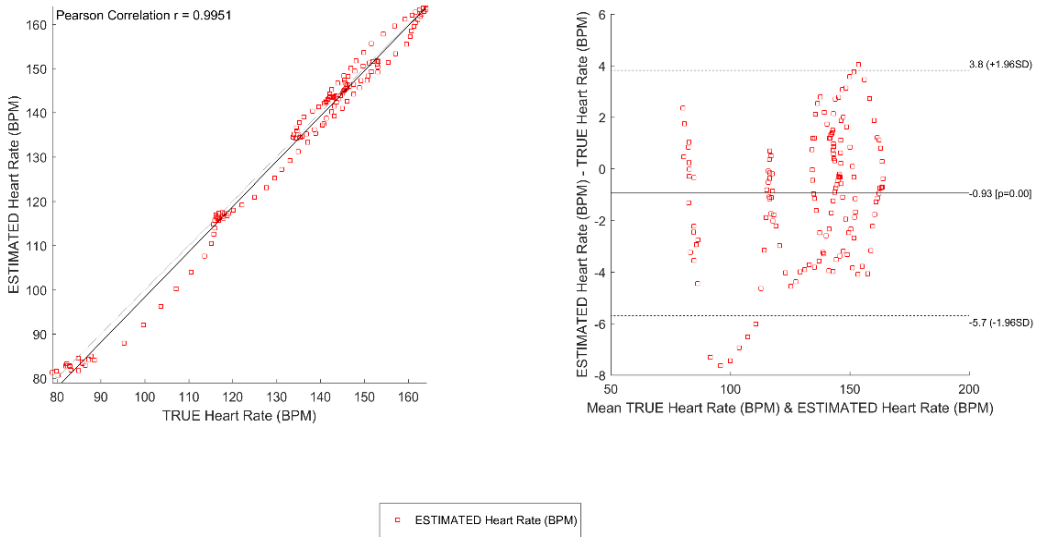

Fig 4: Pearson Correlation and mean value of SUBJECT 4

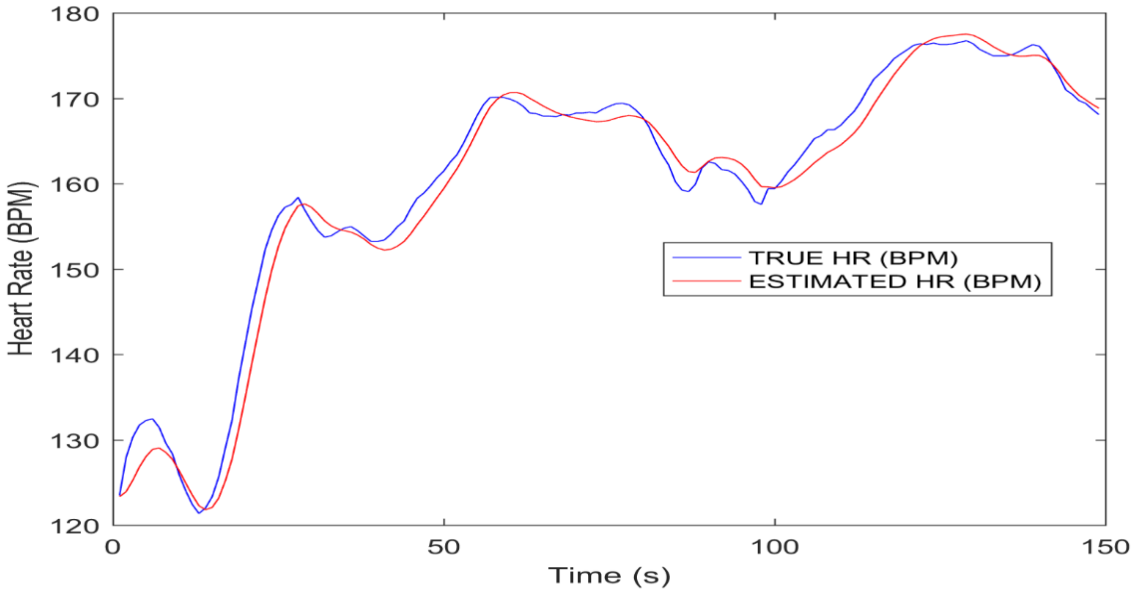

Fig 5: Comparison of estimated HR with ground truth of SUBJECT 10

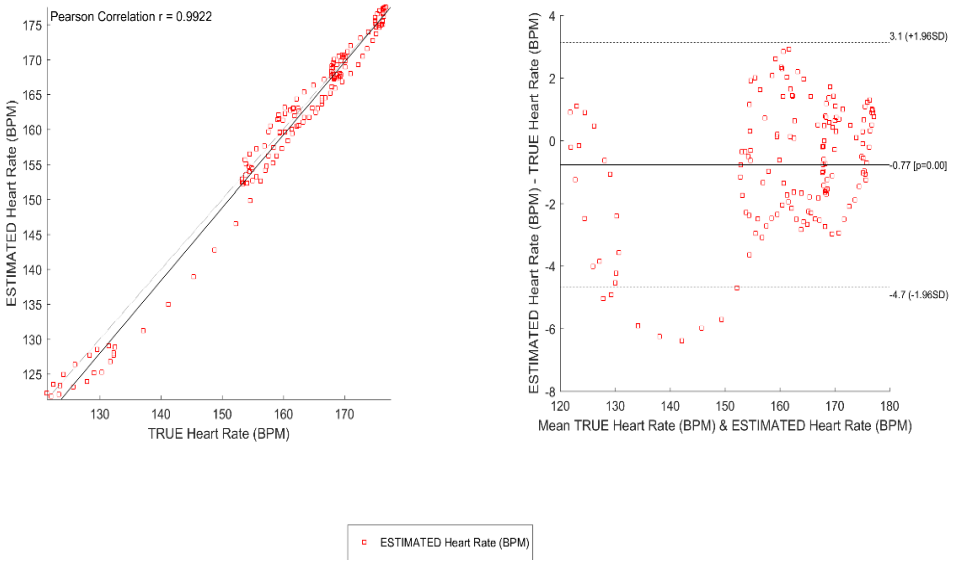

Fig 6: Pearson Correlation and mean value of SUBJECT 10

EP_mae	EP_sdae	EP_mse	EP_rmse	EP_mare	EP_msre	EP_rmsre	EP_mape	EP_mspe	EP_rmspe	FID
0.58683921	0.311494754	0.440753636	0.66389279	0.00490912	3.67E-05	0.006059566	0.490912218	0.367183416	0.605956612	DATA_01_TYPI
0.59263876	0.323947041	0.455453321	0.674872818	0.00529437	4.19E-05	0.006470136	0.529436827	0.418626645	0.647013636	DATA_02_TYPI
0.78697027	0.41282842	0.78853217	0.887993339	0.00635287	5.61E-05	0.007486715	0.635287249	0.560508998	0.748671488	DATA_03_TYPI
0.46376189	0.321597961	0.317791947	0.563730385	0.00392958	2.82E-05	0.005309725	0.392957693	0.281931756	0.530972462	DATA_04_TYPI
0.96354481	0.474743595	1.152256382	1.073432058	0.00702028	6.44E-05	0.008027331	0.702028287	0.644380503	0.802733145	DATA_05_TYPI
0.4269934	0.257815391	0.248349018	0.498346283	0.00366977	2.40E-05	0.004897613	0.366977237	0.239866166	0.489761336	DATA_06_TYPI
0.71885086	0.383089655	0.662477962	0.813927492	0.00566747	4.56E-05	0.006755206	0.566746961	0.456328116	0.675520626	DATA_07_TYPI
0.38808728	0.283006909	0.230204068	0.47979586	0.00342033	2.26E-05	0.004757051	0.342032736	0.226295335	0.475705092	DATA_08_TYPI
0.59816801	0.316116946	0.457064218	0.676065247	0.00512285	3.84E-05	0.006200114	0.512284844	0.384414175	0.620011431	DATA_09_TYPI
0.96495476	0.503976203	1.183425067	1.087853422	0.00614972	5.05E-05	0.007106639	0.6149716	0.505043193	0.71066391	DATA_10_TYPI
0.97332461	0.482006643	1.178066518	1.085387727	0.00655254	5.61E-05	0.007490085	0.655254123	0.561013679	0.749008464	DATA_11_TYPI
0.83407944	0.431472655	0.880582035	0.938393326	0.00620228	5.26E-05	0.00725569	0.620227878	0.526450355	0.725568987	DATA_12_TYPI
0.64856358	0.309926168	0.516012504	0.718340103	0.00889167	9.94E-05	0.009969659	0.889167263	0.993941069	0.996965932	True_S01_T01
0.7032947	0.348277864	0.615035529	0.784242009	0.00942128	0.000112161	0.01059062	0.9421278	1.121612228	1.059061957	True_S02_T01
0.64098434	0.345173815	0.529178485	0.727446551	0.00525153	3.87E-05	0.00622151	0.525152561	0.38707192	0.622151043	True_S02_T02
0.70560143	0.416352045	0.670081947	0.818585333	0.00468741	3.25E-05	0.005697251	0.468741143	0.324586739	0.569725143	True_S03_T02
0.49774577	0.304366028	0.339523745	0.582686661	0.00564244	4.58E-05	0.006769946	0.56424378	0.458321633	0.676994559	True_S04_T01
1.46444532	0.740728677	2.6878466	1.63946534	0.01197032	0.000180174	0.013422886	1.197032241	1.801738645	1.342288585	True_S04_T02
1.28896969	0.632162025	2.058526293	1.434756527	0.00951574	0.000111939	0.010580132	0.951573734	1.119391832	1.058013153	True_S05_T02
0.54863718	0.286560083	0.382497341	0.618463694	0.00630294	5.39E-05	0.007343948	0.630293545	0.539335723	0.734394801	True_S06_T01
0.9760839	0.519408966	1.220625547	1.104819237	0.00694879	6.39E-05	0.007991219	0.694879367	0.638595741	0.799121856	True_S06_T02
1.43335118	0.708449978	2.552249019	1.597575982	0.01131486	0.000159932	0.012646432	1.131486207	1.599322336	1.264643165	True_S07_T02
0.83240694	0.409515255	0.858927035	0.926783165	0.00964934	0.000114722	0.010710847	0.96493378	1.147222444	1.071084705	True_S08_T01

Table 1: Comparing the performance value of various methods in the ISPC dataset

EP_mae	EP_sdae	EP_mse	EP_rmse	EP_mare	EP_msre	EP_rmsre	EP_mape	EP_mspe	EP_rmspe	FID
0.54054054	0.539316503	0.581081081	0.762286745	0.00452535	4.56E-05	0.006754958	0.452535322	0.456294535	0.675495769	DATA_01_TYPE
0.59459459	0.506257951	0.608108108	0.779812867	0.00537704	5.40E-05	0.007346143	0.537704023	0.539658098	0.734614251	DATA_02_TYPE
0.81428571	0.557302267	0.971428571	0.985610761	0.00657658	6.79E-05	0.008240976	0.657658332	0.67913678	0.824097555	DATA_03_TYPE
0.5	0.515283651	0.51369863	0.716727724	0.00420417	3.95E-05	0.006288668	0.420417189	0.395473397	0.628866757	DATA_04_TYPE
0.97260274	0.674104315	1.397260274	1.182057644	0.00719288	8.06E-05	0.0089805	0.719288126	0.806493773	0.898049983	DATA_05_TYPE
0.43333333	0.497195715	0.433333333	0.658280589	0.00360926	3.26E-05	0.005712496	0.360925726	0.326326076	0.571249574	DATA_06_TYPE
0.74825175	0.549885154	0.86013986	0.927437254	0.00586962	5.76E-05	0.007589408	0.586962202	0.575991192	0.758940836	DATA_07_TYPE
0.35625	0.505900716	0.38125	0.617454452	0.00318085	3.37E-05	0.005806735	0.318085068	0.337181662	0.580673456	DATA_08_TYPE
0.61073826	0.502848768	0.624161074	0.790038653	0.00516043	4.83E-05	0.006948125	0.51604345	0.482764414	0.694812503	DATA_09_TYPE
0.95973154	0.6459771	1.33557047	1.155668841	0.00611046	5.60E-05	0.007483996	0.611045569	0.560101958	0.748399598	DATA_10_TYPE
0.96503497	0.643631723	1.342657343	1.158730919	0.00649242	6.30E-05	0.007939453	0.64924206	0.630349198	0.793945337	DATA_11_TYPE
0.79452055	0.631558644	1.02739726	1.013606068	0.00599271	6.39E-05	0.007996705	0.59927111	0.639472956	0.799670529	DATA_12_TYPE
0.62676056	0.499775197	0.64084507	0.800527995	0.00857777	0.000122147	0.011051995	0.857776995	1.221465977	1.105199519	True_S01_T01
0.67153285	0.516058151	0.715328467	0.845770931	0.0089689	0.000127142	0.011275708	0.896890405	1.27141601	1.127570845	True_S02_T01
0.67361111	0.565065268	0.770833333	0.877971146	0.00562502	5.84E-05	0.007639916	0.562502008	0.583683231	0.763991643	True_S02_T02
0.71052632	0.582658658	0.842105263	0.917662935	0.00476096	4.02E-05	0.006338799	0.476095625	0.401803707	0.633879884	True_S03_T02
0.51401869	0.520603532	0.53271028	0.729870043	0.00580876	6.98E-05	0.008355759	0.580875666	0.698187084	0.835575899	True_S04_T01
1.43564356	0.887872081	2.841584158	1.685699902	0.01175947	0.000190992	0.013819999	1.175947415	1.909923601	1.381999856	True_S04_T02
1.25477707	0.758747776	2.146496815	1.465092767	0.00925834	0.00011675	0.010805105	0.925833665	1.167502894	1.080510479	True_S05_T02
0.54545455	0.499826479	0.545454545	0.738548946	0.00616654	7.21E-05	0.008489459	0.616654462	0.720709141	0.8489459	True_S06_T01
1	0.641363795	1.408450704	1.186781658	0.00710966	7.33E-05	0.008559838	0.710966053	0.732708324	0.855983834	True_S06_T02
1.40495868	0.791396576	2.595041322	1.610913195	0.01108378	0.000162638	0.012752944	1.108377641	1.626375826	1.275294408	True_S07_T02
0.81	0.563090319	0.97	0.98488578	0.00937225	0.000128764	0.011347407	0.937224696	1.287636517	1.134740727	True_S08_T01

Table 2: Comparing the performance value of various methods in the ISPC dataset

CONCLUSION:

Wireless sensors used in wrist-worn devices have been compressed for efficient heart rate monitoring. Estimating the heart rate when a person is exercising because of many variations in the heart rate, by incorporating these changes and developing a model is quite challenging. These signals are highly arbitrary and consist of motion artefacts, they act as a substitute to the ECG signal. Here we have proposed an algorithm for efficient feature extraction, preprocessing that data and reducing motion artefacts to estimate accurate heart rate. We have proposed a deep learning technique to efficiently sense the heart rate from the PPG signal, which is collected in ambulant conditions. The PPG signal is extracted from the ECG signal, which is extracted from devices via IoT. We have checked the performance of our model in comparison with the ground truth value. Our model can be extended to accommodate new changes by including new models.

Conflict of interest: The authors declare no conflict of interest.

REFERENCES:

1. Jermana L. Moraes, Matheus X. Rocha, Glauber G. Vasconcelos, José E. Vasconcelos Filho, Victor Hugo C. de Albuquerque and Auzuir R. Alexandria. Advances in

Photoplethysmography Signal Analysis for Biomedical Applications. Sensors (Basel) Vol.18 Issue 6 2018 pp1894.

2. Vescio, Basilio & Salsone, Maria & Gambardella, Antonio & Quattrone, Aldo. "Comparison between Electrocardiographic and Earlobe Pulse Photoplethysmographic Detection for Evaluating Heart Rate Variability in Healthy Subjects in Short- and Long-Term Recordings". Sensors. 18. 2018 pp. 844.
3. A. Temko, "Accurate Heart Rate Monitoring During Physical Exercises Using PPG.," IEEE Trans. Biomed Eng, vol. 64, no. 9, pp. 2016–2024,2017.
4. E. Khan et al., "A Robust Heart Rate Monitoring Scheme Using Photoplethysmographic Signals Corrupted by Intense Motion Artifacts," IEEE Trans. Biomed. Eng., v.63, pp. 550-562, 2016.
5. D. Biswas et al., "Low-Complexity Framework for Movement Classification Using Body-Worn Sensors," IEEE Trans. on Very Large-Scale Int. (VLSI) Sys., vol. 25(4), pp.1537-1548, 2017.
6. D. Zhao et al., "Sfst: A robust framework for heart rate monitoring from photoplethysmography signals during physical activities," Biomedical Signal Processing and Control, vol. 33, pp. 316–324, 2017.
7. D. Biswas et al., "Low-Complexity Framework for Movement Classification Using Body-Worn Sensors," IEEE Trans. on Very Large-Scale Int. (VLSI) Sys., vol. 25(4), pp.1537-1548, 2017.
8. C. J. Dondzila et al., "Congruent accuracy of wrist-worn activity trackers during controlled and free-living conditions," Int. J. Exerc. Sci., vol. 11, no. 7, pp. 575–584, 2018.
9. S. Mehrang, J. Pietilä, and L. Korhonen, "An activity recognition framework deploying the random forest classifier and a single optical heart rate monitoring and triaxial accelerometer wristband," Sensors, vol. 18, no. 2, p. 613, 2018.
10. Y. Zhang et al., "Motion artefact reduction for wrist-worn photoplethysmograph sensors based on different wavelengths," Sensors, vol. 19, no. 3, p. 673, Feb. 2019.
11. M. Essalat, M. B. Mashhadi, and F. Marvasti, "Supervised heart rate tracking using wrist-type photoplethysmographic (PPG) signals during physical exercise without simultaneous acceleration signals," in Proc. IEEE Global Conf. Signal Inf. Process., Dec. 2016, pp. 1166–1170.
12. V. Jindal, "MobileSOFT: U: A deep learning framework to monitor heart rate during intensive physical exercise," Univ. Texas, Dallas, TX, USA, Tech. Rep., 2018
13. A. G. Bonomi et al., "Atrial fibrillation detection using photoplethysmography and acceleration data at the wrist," in Proc. Comput. Cardiol. Conf. (Cin C), Sep. 2016, pp. 277–280.
14. M. Lemay et al., "Wrist-located optical device for atrial fibrillation screening: A clinical study on twenty patients," in Proc. IEEE Comput. Cardiol. Conf. (Cin C), Vancouver, BC, Canada, Sep. 11–14, 2016, pp. 681–684. doi: 10.23919/CIC.2016.7868834.

15. S. P. Shashikumar, A. M. Shah, Q. Li, G. D. Clifford, and S. Nemati, “A deep learning approach to monitoring and detecting atrial fibrillation using wearable technology,” in Proc. IEEE EMBS Int. Conf. Biomed. Health Inform. (BHI), Feb. 2017, pp. 141–144.
16. A. G. Bonomi et al., “Atrial fibrillation detection using photoplethysmography and acceleration data at the wrist,” in Proc. Comput. Cardiol. Conf. (Cin C), Sep. 2016, pp. 277–280.
17. M. Lemay et al., “Wrist-located optical device for atrial fibrillation screening: A clinical study on twenty patients,” in Proc. IEEE Comput. Cardiol. Conf. (Cin C), Vancouver, BC, Canada, Sep. 11–14, 2016, pp. 681–684. doi: 10.23919/CIC.2016.7868834.
18. S. P. Shashikumar, A. M. Shah, Q. Li, G. D. Clifford, and S. Nemati, “A deep learning approach to monitoring and detecting atrial fibrillation using wearable technology,” in Proc. IEEE EMBS Int. Conf. Biomed. Health Inform. (BHI), Feb. 2017, pp. 141–144.
19. T. Rault, A. Bouabdallah, Y. Challah, and F. Marin, “A survey of energy-efficient context recognition systems using wearable sensors for healthcare applications,” Pervasive Mobile Comput., vol. 37, pp. 23–44, Jun. 2017.
20. S. M. Riazul Islam, D. Kwak, M. Humayun Kabir, M. Hossain, and K.-S. Kwak, “The Internet of Things for health care: A comprehensive survey,” IEEE Access, vol. 3, pp. 678–708, 2015.
21. B.-S. Lin, A. M. Wong, and K. C. Tseng, “Community-based ECG monitoring system for patients with cardiovascular diseases,” J. Med. Syst., vol. 40, no. 4, p. 80, Apr. 2016.
22. D. G. Benditt, W. O. Adkisson, R. S. Sutton, R. K. Mears, and S. Sakaguchi, “Ambulatory diagnostic ECG monitoring for syncope and collapse: An assessment of clinical practice in the United States,” Pacing Clin. Electrophysiol., vol. 41, no. 2, pp. 203–209, 2018
23. T. Y. Satheesha, D. Satyanarayana, M. N. G. Prasad and K. D. Dhruve, "Melanoma Is Skin Deep: A 3D Reconstruction Technique for Computerized Dermoscopic Skin Lesion Classification," in IEEE Journal of Translational Engineering in Health and Medicine, vol. 5, pp. 1-17, 2017, Art no. 4300117, doi: 10.1109/JTEHM.2017.2648797.
24. S. Aich, K. Young, K. L. Hui, A. A. Al-Absi and M. Sain, "A nonlinear decision tree-based classification approach to predict the Parkinson's disease using different feature sets of voice data," 2018 20th International Conference on Advanced Communication Technology (ICACT), 2018, pp. 1-2, doi: 10.23919/ICACT.2018.8323863.
25. Munivenkatappa, Nagabushanam & Prasanna, Cyril & P, Raj & Ramachandran, Saravanan. (2009). Design and Implementation of Parallel and Pipelined Distributive Arithmetic Based Discrete Wavelet Transform IP Core. 35.